ISMRM 14th SCIENTIFIC MEETING & EXHIBITION, Seattle, Washington, USA, May 6-12, 2006

Spectral Separation Analyses of Proton MRSI Data: Validation with Tumor Grade of Brain Glioma

Sunitha B. Thakur[1], Yuzhuo Su[2], Karimi Sasan[1], Shuyan Du[3], Paul Sajda[3], Wei Huang[1], Lucas C. Parra[2].

[1]Neuroradiology, Memorial Sloan-Kettering Cancer Center;
[2]Biomedical Engineering Department, City College of New York, Program in Engineering, the Graduate Center, City University of New York;
[3]Department of Biomedical Engineering and Department of Radiology, Columbia University;

Introduction

In vivo ^{1}H magnetic resonance spectroscopic imaging (MRSI) can provide regional characterization and quantification of molecular markers in tissue, and has been widely used for improving diagnosis and treatment monitoring of a variety of neuro-pathologies, most notably brain cancers (1). In clinical settings, because of limitation in scanning time for data averaging, the average MRSI voxel size is about 1 cc in order to achieve reasonable signal-to-noise ratio. Due to the heterogeneous nature of the tumor tissue, the relatively large voxel may encompass a mixture of normal brain tissue and infiltrating tumor tissue (partial volume effect). This often leads to significant variability in spectral pattern and limits diagnostic potential of MRSI for brain tumors, such as tumor grading and determination of tumor spatial expansion.

Previously, Sajda et al. (2) proposed an algorithm called constrained non-negative matrix factorization (NMF) that extracts constituent spectra associated with different tissue types by simultaneously analyzing all voxel spectra. In principle this method solves the partial volume effect as it determines also the proportion with which each constituent spectrum contributes to an individual voxel spectrum. In this preliminary study, this spectral separation algorithm was applied to the clinical MRSI data of brain gliomas. The goal was to validate this MRSI data analysis method by correlating the analysis results with pathologically proven tumor grades.

Methods

IRB waiver was obtained to retrospectively analyze the clinical proton MRSI data and examine the medical records of 14 patients who had pathologically proven brain gliomas. Among them, 7 had grade I/II and 7 had grade III/IV. Based on clinical standards, grade I/II glioma is categorized as low grade glioma (LGG), while grade III/IV glioma is categorized as high grade glioma (HGG).

As part of a clinical brain tumor MRI/MRS protocol, the 3D MRSI scans were performed on a GE 1.5T LX or Excite scanner using the commercial PRESS sequence, with TE = 144 ms, TR = 1000 ms, FOV = 8 cm, 1 cm slice thickness, and 8x8x8 phase encoding matrix size, resulting in 8.5 min scanning time and 1 cc nominal voxel size. Prior to MRSI acquisition, FLAIR scout images were collected for prescribing MRSI acquisition. Raw time-domain MRSI data and FLAIR images were imported into a home-built program (3) that incorporates the NMF algorithm. The program performed the general spectroscopic processing procedures such as Fourier transformation, baseline and phase corrections, frequency alignment, etc. and generated conventional MRSI spectra. These multi-voxel spectra were then overlaid onto the FLAIR images and the results were validated with those obtained using GE's Functool software for MRSI data processing.

Following the validation, all voxel spectra were submitted to the NMF algorithm for spectral separation analysis. In this study, for each patient's MRSI data set, the algorithm represented each voxel's spectrum as a linear combination of spectra from tumor tissue, normal brain tissue, and residual baseline activity. The constituent spectra are consistent across all the MRSI voxels, while the coefficients of the linear relationship are different for each voxel, representing the abundance of each constituent tissue.

Results

Fig. 1 demonstrates the typical process of the MRSI data analysis. The left panel shows the conventionally processed MRSI multi-voxel spectra overlaid onto a FLAIR image with areas of hyperintensity indicating the tumor region (this patient had high grade fibrillary astrocytoma). The white box represents the region of RF excitation, which was smaller than the FOV of MRSI acquisition. The center panel shows the results of NMF analysis: the constituent spectra of the normal tissue, tumor tissue, and residuals. The constituent tumor spectrum revealed typical pattern of high choline-compounds (Cho) level but low N-acetylaspartate (NAA) level. The right panel shows the tumor/normal tissue abundance map overlaid onto the FLAIR image: the redder the area, the more abundant the tumor tissue; the bluer the area, the more abundant the normal tissue.

Fig. 2a shows the Cho versus NAA plot in arbitrary units of the data points from all the patients, taken from the individual MRSI voxels located in the regions of FLAIR hyperintensity and surrounding normal appearing areas before the NMF analysis. As shown in the plot, there is significant overlap in voxel spectral pattern between the HGG, LGG, and the normal appearing regions due to partial volume effect, making diagnosis difficult. Fig. 2b shows the same type of plot of the constituent tumor and normal tissue spectra from all 14 patients following the NMF analysis. The Cho-NAA patterns of the normal spectra were well separated from those of the tumor spectra. Cho levels were significantly ($p < 0.007$, $r = -0.69$) correlated with NAA levels with the HGGs generally showing higher Cho and lower NAA levels than the LGGs.

Discussion

In this preliminary study, the spectral patterns (Cho level versus NAA level) of the constituent tumor spectra generated by the NMF algorithm analyses of the clinical 3D MRSI data are consistent with the grade of brain gliomas, suggesting this method has the potential for clinical applications. By resolving the partial volume effect, the NMF analysis reduces variability of *in vivo* spectra. Furthermore, by measuring regional abundance of tumor and normal tissue, this algorithm can be particularly useful in defining tumor margins, treatment planning of radiation therapy (4), and surgical decisions.

References 1. Pirzkall A et al., Int. J. Rad. Oncology Bio. Phys. **53**, 1254 (2002). 2. Sajda P et al., IEEE Trans. Med. Imaging **23**, 1453 (2004). 3. Su Y et al., Ann. Metg. BME Soc. (2005). 4. Graves EE et al., Image Anal. Stereol. **21**, 69 (2002).

Fig. 1

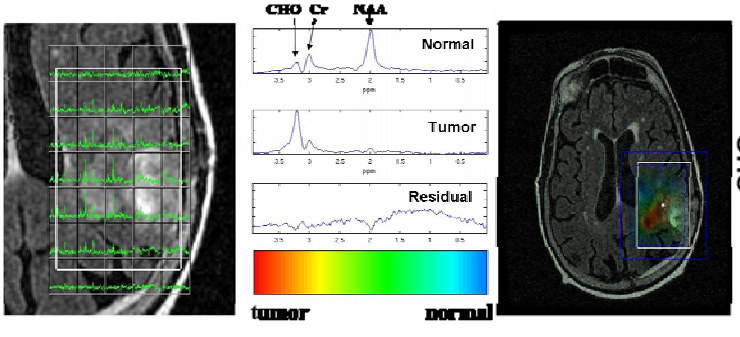

Fig. 2a

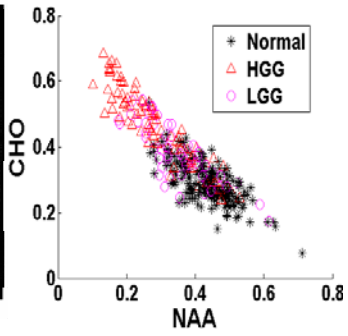

Fig. 2b